A Segmentation Method Using Multiscale and Multidirectional Matched Filters Based on Dyadic Wavelet Transform for Finger Vein Pattern Extraction

Marios Vlachos[*1], Evangelos Dermatas[2]

Department of Electrical Engineering & Computer Technology, University of Patras, Patras, 26500, Hellas

[*1]mvlachos@teemail.gr; [2]dermatas@george.wcl2.ee.upatras.gr

Abstract

In this paper an efficient automatic method for robust segmentation of finger vessel-network and vein pattern extraction from infrared images acquired by a low-cost monochrome or multichannel camera, is proposed. After brightness normalization, the fingerprint lines are eliminated using the 2D dimensional discrete wavelet transformation. A set of twelve directional kernels is constructed, based on a dyadic wavelet transform, for each scale and is used to enhance the directional properties of veins. From maximum filters' response along scale and direction, a neighborhood thresholding derives a binary segmented image to produce reliable patterns of finger veins. A post-processing module is used in case where low-quality images are to be segmented. Preliminary evaluation experiments of the proposed method demonstrate a number of advantages, compared to recently published methods.

Keywords

Finger Vein Pattern; Fingerprint Lines; Dyadic Wavelet; Steerable Filters; Matched Filter

Introduction

The problem of finger vein extraction arises mainly in biometric applications but it is also very important for the biomedical research community. In a few number of studies, due to the recent scientific interest in this area, vein enhancement methods in infrared images have been presented. An important applications area is related to human verification and recognition, including a wide range of systems such as area-access control, PC login, and e-commerce. The main advantage over the other conventional verification methods such as keys, passwords and PIN numbers is that vein pattern verification does not suffer from thefts, loss and reliance on the user's memory. The measurement of human biological attributes including fingerprint, face, iris, retina, voice and hand geometry recognition do not insure necessarily confidentiality, because the features are exposed outside the human body. A biometric system which uses patterns of veins overcomes the above problems due the patterns of veins are inside the human body. Vein or vessel extraction is also very useful in biomedical imaging, vascular pathology, improving diagnosis and follow-up of angiogenesis in the human body. Inspection of the retinal vasculature may reveal hypertension, diabetes, arteriosclerosis, cardiovascular disease, stroke, and glaucoma, the second commonest cause of blindness in West-countries and the commonest cause of blindness worldwide.

An application specific processor for vein pattern extraction, and its application to a biometric identification system, is proposed by Park et al. (1997), consisting of three sequential processes, finger detection in the original infrared image, image-enhancement, and veins detection. The last two processes are the most time consuming parts of the complete method. The image-enhancement consists of a Gaussian low-pass filter, a high-pass filter, and a modified median filter. Consequently, low pass spatial filtering is used for noise removal, and high pass spatial filtering for emphasizing vascular patterns, followed by thresholding [Park et al. (1997), Hong et al. (1999), Im et al. (2001)].

An improved vein pattern extracting method is proposed by Im et al. (2000), compensating the loss of vein patterns in the edge area, giving more enhanced and stabilized vein pattern information, giving better performance than similar methods. The problem arising from the iterative nature of the image-enhancement filters is solved by designing a filter that is processed only ones, giving fast extraction of vein

patterns and reduced hardware complexity. The fa1se acceptance rate in verification experiments is five times better than existing algorithm and the processing speed is measured to be 100 ms/image.

Im et al. (2003), implement a vascular pattern extraction algorithm, based on the directional information of vascular patterns using two filters: a row-pattern filter for abscissa vascular pattern extraction and a column-pattern filter for effective extraction of the ordinate vascular patterns. The combined output produces the vascular patterns in hand images. Unlike the conventional hand vascular pattern extraction algorithm, the directional extraction approach prevents loss of the vascular pattern connectivity.

A method for personal identification, based on finger vein patterns, is presented and evaluated by Miura et al. (2004), using line tracking starting at various positions. Local dark lines are identified and a pixel based line tracking algorithm is executed by moving along the lines.

A method for finger vein pattern extraction in infrared images is proposed by Vlachos et al. (2006). Using image enhancement and kernel filtering methods, the vein patterns in low contrast images are detected. Further improvement is achieved by a two-level morphological process: a majorities-filter smoothes the contours and removes some of the misclassified isolated pixels, followed by a reconstruction procedure used to remove the remaining misclassified regions.

Tanaka et al. (2004), propose a certification system comparing vein images for low-cost, high speed and high precision certification. The recognition algorithm is based on phase correlation and template matching. Several noise reduction filters, sharpness filters and histogram manipulations are tested, giving a high certification ratio.

Ding et al. (2005), study the theoretical foundation and difficulties of hand vein recognition are introduced and threshold segmentation and line-thinning method in hand vein images. As a result, a new segmentation method and an improved conditional thinning method are proposed, followed by a feature extraction method based on end-points and crossing-points. The 99.1% pass ratio using distance measures in human verification experiments is achieved.

Preliminary work and experiments for localizing surface veins via near-infrared (NIR) imaging and structured light ranging are presented by Paquit et al. (2006). The eventual goal of the system is to serve as the guidance for a fully automatic catheterization device. A NIR line-generating LED module is used to implement structured light ranging and construct a 3D topographic map of the arm surface. The located veins are mapped to the arm surface to provide a camera-registered representation of the arm and veins.

A Vein Contrast Enhancer (VCE) has been constructed by Zeman et al. (2002, 2004) to facilitate the vein access by capturing an infrared image of veins, enhancing the contrast, and projecting the vein image back onto the skin. The VCE also aligns the projected image with the vein very accurately with a divergence of 0.06mm.

Several studies had described the problem of extracting or enhancing directional information using rotation-invariant operators [Freeman et al. (1991), Mallat et al. (1992)]. Freeman et al. (1991), proposed the concept of steerable filters and tested in several image segmentation applications.

In this paper a novel method to enhance infrared images of finger in order to segment the vessel network and extract the corresponding vein pattern is presented. Three main processes are involved: multiscale and multidirectional vein enhancement, automatic segmentation by local neighborhood thresholding and vein pattern extraction by morphological postprocessing. The local thresholding method is selected due to its simplicity and its ability to robustly segment the image of the finger in two regions: vein and tissue which is the desired goal. In case of high quality images some of the processing elements such as preprocessing and postprocessing can be skipped, which results in a significant reduction in computational complexity.

The structure of this paper is as follows: In the following section, a detailed description of the proposed method is given, followed by the experimental evaluation and comparison, presented in the last section.

Extraction of Finger Veins

The hardware used to acquire the IR images consisting of an array of infrared leds, an inexpensive CCD camera, and a low-cost frame-grabber. The finger was placed between the camera and the light source, consisting of a row of infrared leds (five elements) with adjustable illumination. The leds intensity is controlled by a voltage regulator to produce the appropriate illumination, taking into account the

exposure time, the finger thickness, and the color of the skin. Excellent illumination conditions facilitate the forthcoming digital processing methods, but the accuracy of the vein extraction process is insensitive to small variations in the illumination conditions, as the experimental results show. Due to the fact that haemoglobin has strong absorption in the infrared wavelengths than the other parts of the human body i.e. tissue, the veins are reached in the darker areas. So, the goal of our study is to extract the dark vein regions from the background. An original digital image, acquired by the described hardware is shown in FIG. 1 a.

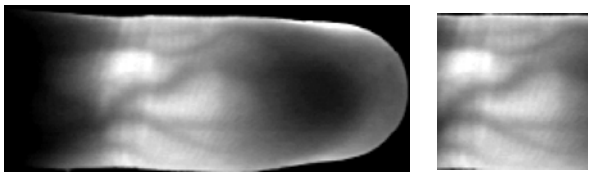

a. b.

FIG. 1 a. ORIGINAL DIGITAL IMAGE AND FIG. b. ROI IMAGE

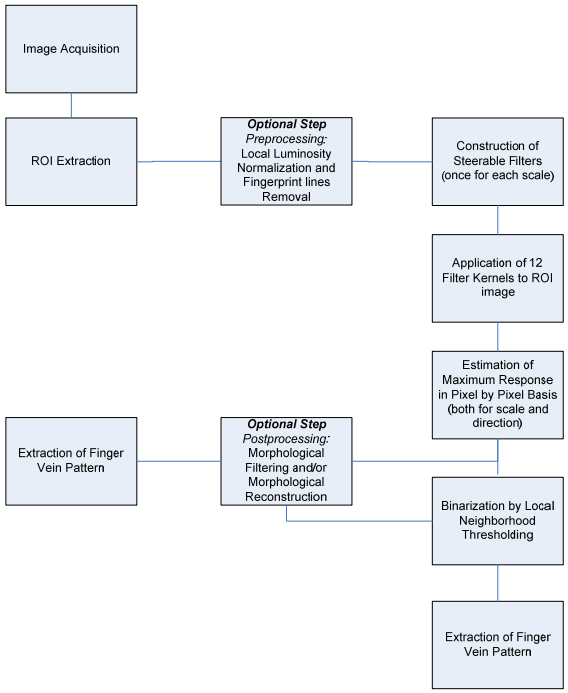

FIG. 2 FLOWCHART OF PROPOSED FINGER VEIN EXTRACTION METHOD IN INFRARED IMAGES

From the original digital image, a region of interest (ROI) is automatically extracted for further processing, isolating the finger and detecting the finger areas containing vein patterns. The ROI is shown in FIG. 1 b. The proposed method consists of a sequence of processes presented in detail in the following subsections. FIG. 2 shows the flowchart of the proposed method.

Preprocessing

In case of low contrast, poor illumination conditions, and/or noisy infrared images, a preprocessing module enhances the image properties to obtain the desirable quality. This preprocessing module is especially useful for correcting non-uniform illumination or shading artifacts. The local linear-normalization process adapts the image brightness taking into account the statistical properties of the neighbor pixels, as shown in FIG. 3. The linear transformation parameters, window sizes, w_1, and, w_2, are derived experimentally and are close related to the local mean and variance.

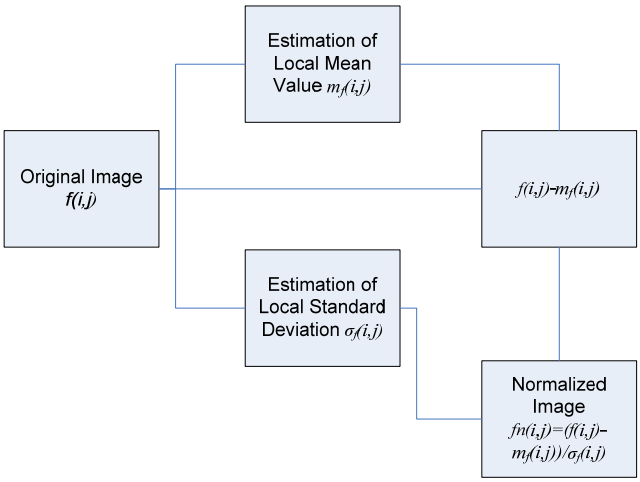

FIG. 3 THE BLOCK DIAGRAM OF THE LOCAL NORMALIZATION PROCEDURE

The normalized image f_n is estimated inside the ROI as follows:

$$f_n(i,j) = \frac{f(i,j) - m_f(i,j)}{\sigma_f(i,j)}, \qquad (1)$$

where $f(i,j)$ is the original image, and $m_f(i,j)$, $\sigma_f(i,j)$ is an estimation of the mean, and standard deviation of the neighbor pixels respectively. The estimation of the mean and standard deviation is performed using spatial smoothing. The sizes of the windows are the parameters of this process.

Elimination of Fingerprint Lines

Although, after local normalization the image has satisfactory contrast, the fingerprint lines are still visible and can erroneous classified as veins. In typical human fingers, the fingerprint lines are perpendicular to vein lines. Robust reduction of fingerprint lines can be achieved using the two dimensional discrete wavelet transform [Gongalez et al. (2003)]. The optimum decomposition level depends on the distance

between CCD and finger, and the optical system. Extended experiments at different decomposition levels of wavelet transform from one to five have shown that the presence of fingerprint lines can be separated and therefore can be eliminated with a very low influence to the tissue and vein patterns.

After the application of the two dimensional discrete wavelet transformation and the observation of the approximation and detail coefficients, it is evident that from the detail coefficients these that hold the main information about fingerprint lines are the vertical and diagonal. Although, the horizontal coefficients hold also this information, they remain unchanged because the cut off of these coefficients may result in a possible loss of the information of veins, since the majority of veins tend to guide also in horizontal direction.

The reconstruction of the image after the cut off process is implemented using the two dimensional discrete inverse wavelet transform [Gongalez et al. (2003)]. In substance, the process of cut off the detail vertical and diagonal coefficients in all three decomposition levels is equal to cut off the fingerprint vertical and diagonal lines in the adjusted image.

In [Vlachos et al. (2006)], a detailed presentation of the fingerprint lines elimination process is given. The ROI image after fingerprint elimination is shown in FIG. 4 b and is denoted as *g*.

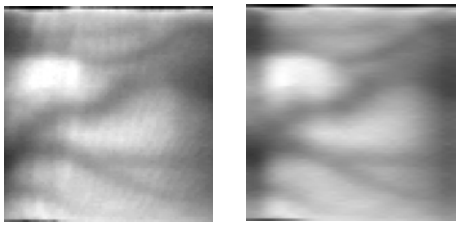

a. b.

FIG. 4 a. ROI IMAGE, FIG. b. ROI IMAGE AFTER FINGERPRINT LINES ELIMINATION

Construction of Steerable Filters

If W_{xL} and W_{yL} are the wavelets transforms of *x* and *y* direction at level-*L*, any linear expression of W_{xL} and W_{yL} setup the wavelet transform in the arbitrary direction θ: $W_{\theta L} = W_{xL}\, cos(\theta) + W_{yL}\, sin(\theta)$.

The Gaussian function is one of the mother wavelets:

$$G(i, j) = \frac{1}{2 \cdot \pi \cdot \sigma^2} \cdot \exp\left(-\frac{(i^2 + j^2)}{2 \cdot \sigma^2}\right) \qquad (2)$$

and its derivatives can be used to characterize the image brightness in different regions [Mallat et al. (1992)]. So, it is reasonable to select the second derivatives of the Gaussian function for detecting and enhancing the finger veins. The directional derivatives of the two dimensional Gaussian function *G(i,j)*, with zero mean and variance σ^2 are:

$$Q_x(i, j) = -\frac{i}{\sigma^2} G(i, j) \qquad Q_y(i, j) = -\frac{j}{\sigma^2} G(i, j). \quad (3)$$

The two-dimensional dyadic wavelet transform in horizontal and vertical direction at scale *L* is given by:

$$W_{xL} \cdot g(i, j) = g(i, j) * \psi_{xL}(i, j) \text{ and}$$

$$W_{yL} \cdot g(i, j) = g(i, j) * \psi_{yL}(i, j), \qquad (4)$$

where

$$\psi_{xL}(i, j) = \frac{1}{4^L} \cdot Q_x\left(\frac{i}{2^L}, \frac{j}{2^L}\right),$$

$$\psi_{yL}(i, j) = \frac{1}{4^L} \cdot Q_y\left(\frac{i}{2^L}, \frac{j}{2^L}\right). \qquad (5)$$

According to the steerability principle, the arbitrary direction θ wavelet transform at scale *L* is given by:

$$W_{\theta L} = W_{xL} \cdot \cos\theta + W_{yL} \cdot \sin\theta = g(i, j) * (\psi_{xL} \cdot \cos\theta + \psi_{yL} \cdot \sin\theta)$$

or

$$W_{\theta L} = W_{xL} \cdot \cos\theta + W_{yL} \cdot \sin\theta = g(i, j) \cdot V(i, j, \theta), \quad (6)$$

where $V(i, j, \theta) = \psi_{xL} \cdot \cos\theta + \psi_{yL} \cdot \sin\theta$, (7)

and * denotes convolution with the preprocessed image *g*.

Multiple Direction Image Filtering

Twelve different filter kernels are constructed for each scale by selecting twelve different values for the angle which forms the orientation of filter kernel with the horizontal axis (FIG. 5). The kernel size is strongly correlated with the average vein diameter. If the average vein diameter in the acquired image is *n* the minimum filter kernel size must be $2 \cdot n + 1$. The values of θ were set to 0, 15, 30, 45, 60, 75, 90, 105, 120, 135, 150 and 165 degrees. These values are proved experimentally sufficient to represent the majority of possible vein orientations. The preprocessed image was convolved sequentially with the twelve different kernels. The twelve responses are shown in FIG. 6. In applications where the execution time is extremely crucial, the number of filter kernels can be decreased to six without significant reduction in the method's accuracy.

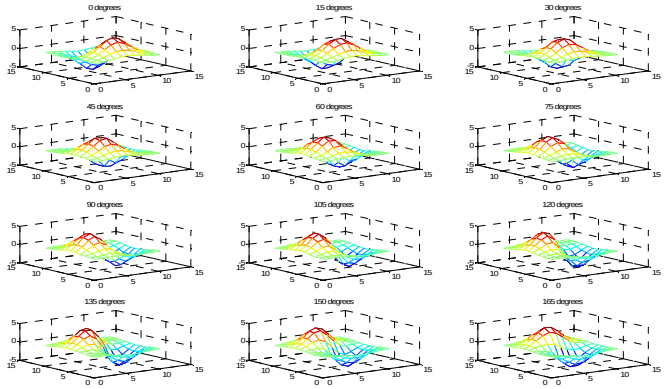

FIG. 5 THE TWELVE FILTER KERNELS CONSTRUCTED FOR VARIOUS ANGLES θ

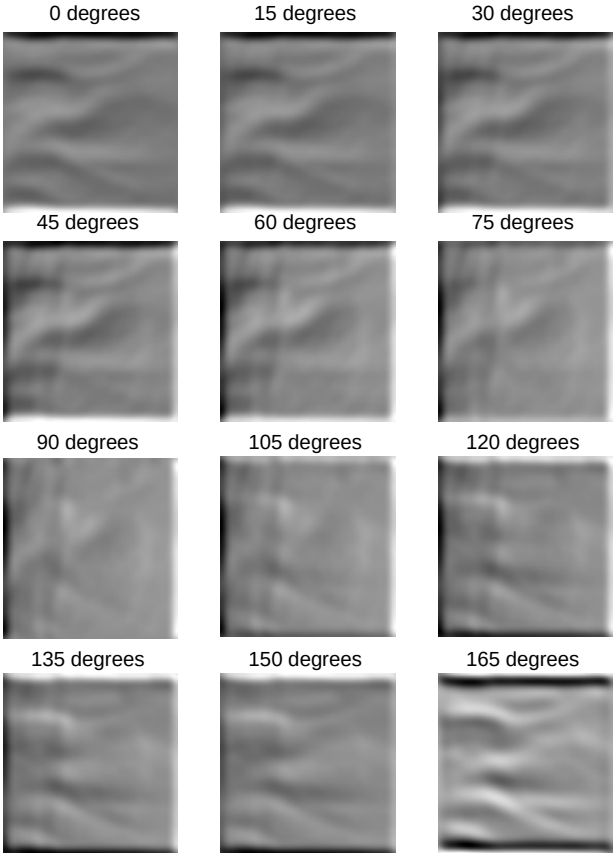

FIG. 6 THE TWELVE DIRECTIONAL RESPONSES

Initial Construction of Veins Map

The advantages of multiscale edge representation are used to construct the initial veins map and the most effective scale factor is derived, maximizing the separation capabilities of wavelet analysis. Taking into account that the veins thickness varies and the image resolution differs (related to the imaging system), multiple maximum response images for a number of scales are estimated and the initial veins map is constructed from the maximum response of these images.

In the final stage of this procedure, brightness normalization is implemented to face the scaling effect; the maximum responses in different scales differ significantly. The adopted normalization process unifies the first two statistical properties, setting the mean value of the brightness values to zero and the corresponding variance to one. Thus, the equivalent linear transformation of brightness for each pixel is given by the following formula:

$$\mathrm{Im}\,n_L = \frac{\mathrm{Im}_L - mean(\mathrm{Im}_L)}{std(\mathrm{Im}_L)}, \tag{8}$$

where Im_L is the maximum response along different directions and at scale L before the normalization:

$$\mathrm{Im}_L = \max_{\theta} W_{\theta L}, \tag{9}$$

$\mathrm{Im}\,n_L$ is the normalized maximum response at scale L, and $mean(\mathrm{Im}_L)$, $std(\mathrm{Im}_L)$ are the mean value and the standard deviation of the maximum response at scale L.

After the linear transformation, the estimation of the total maximum response along scales can be readily achieved using the following equation:

$$Igm = \max_{L}(\mathrm{Im}\,n_L). \tag{10}$$

The total maximum along the scales, estimated in a pixel basis, is used to construct the total multiscale and multidirectional maximum response image. In the total maximum response image, the veins have been enhanced and the local neighborhood thresholding which follows can easily discern them from the surrounding tissue. FIG. 7 b shows the total maximum response image.

Even though, in the application of the proposed method to real infrared images it was not necessary to perform multiscale analysis because the average vein's diameter did not vary significantly and it was almost constant along the finger. However, multiscale analysis still is mentioned since the proposed method does not restrict only in the presented application but it could be applied in a variety of image processing and computer vision applications (i.e. road extraction from satellite images, retinal vessel segmentation e.t.c). In such applications the multiscale version of the proposed method might be inevitable.

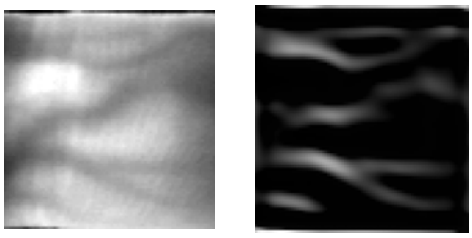

a. b.

FIG. 7 a. ROI IMAGE, FIG. b. TOTAL MAXIMUM RESPONSE IMAGE

Local Neighborhood Thresholding

The local neighborhood thresholding is a simple and computational efficient process for segmenting images, in contrast to the global thresholding Otsu's method [Otsu (1979)] which proved inadequate in our experiments.

In every pixel, a square window of *nxn* pixels, containing the neighbor pixels is considered (the testing pixel is the centre of window), and the mean value of the pixels brightness inside the window is estimated. If the brightness of the central pixel is greater than the corresponding mean value, the pixel is considered as vein, otherwise it is considered as tissue, as shown in FIG. 8 a. The window size affects significantly the quality of the produced binary image, and the most effective window size is selected experimentally.

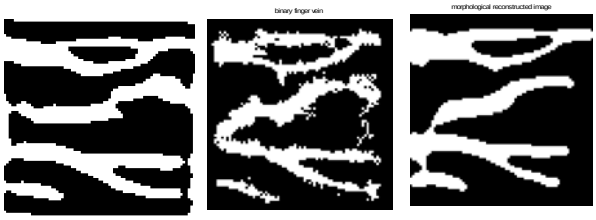

a. b. c.

FIG. 8 FINGER VEIN PATTERN USING FIG. a. THE PROPOSED METHOD , FIG. b. THE METHOD DESCRIBED IN [Miura et al. (2004)], AND FIG. c. THE METHOD DESCRIBED IN [Vlachos et al. (2006)]

Postprocessing

As shown in FIG. 8 a, the segmentation result is adequate to describe the finger veins and does not require further processing. However, in some cases, the original image suffers from low-contrast and strong noise presence, so the segmentation result may not satisfy the desired specifications. In such cases, some misclassification areas appear as isolated circular or shapeless regions which generally do not associate with veins. Thus, a post-processing step is required. In our study, morphological filtering and/or morphological image reconstruction process is used to eliminate the erroneous regions [Vlachos et al. (2006)]. As mentioned, the use of the preprocessing or the postprocessing modules depends on the specific image characteristics.

Experimental Results

The experimental evaluation of the proposed method is carried out using both a real and an artificial finger image database containing each 10 images. In our experiments the acquired images satisfy the expected quality and the proposed preprocessing step is not used. The optimum value of the window's size in the local thresholding process is derived experimentally, and it is set to 31x31 pixels for the real image database.

In low cost imaging systems, typical configuration of these systems includes a pinhole lens, 3 cm distance between CCD and finger, and a monochrome 640 x 480 pixels CCD. In this hardware configuration, the best approximation and detail (horizontal, vertical and diagonal) wavelet-decomposition for fingerprint elimination are achieved using the coefficients in three levels (cA_3, cH_1, cH_2, cH_3, cV_1, cV_2, cV_3, cD_1, cD_2, cD_3) by means of a member from the biorthogonal (bior3.7) family, producing satisfactory separation of the fingerprint lines, ensuring also the property of linear phase for accurate image reconstruction.

An experimental evaluation and comparison between the proposed method, using only the first scale wavelet analysis in the initial construction of the vein map, and similar methods [Miura et al. (2004), Vlachos et al. (2006)] are carried out in the complete set of images. In FIG. 8 the most representative differences are shown for the extracted finger vein patterns. Although the lack of quantitative results, the proposed method seems to be more effective than the other two and it succeeds to identify veins in difficult regions where the others fail. Furthermore it prevents connectivity, as the method presented in [Vlachos et al. (2006)] also does, while the method described in [Miura et al. (2004)] could not always guarantee it. Moreover, in the majority of the acquired images, the proposed method does not require a preprocessing step while other methods usually required it.

Artificial Image Database

A quantitative evaluation of the proposed method in real infrared images is difficult due to the absence of manual segmentation data. The extremely low

contrast images increase the disagreement of human annotation. Therefore, the proposed method is evaluated using a small set of images each of which is created by the weighed sum of the two artificial images. The first image is constructed using an artificial vein-like network. This network consists of connected lines of different widths with junctions and bifurcations and multiple low pass filtering to simulate the blurriness of the edges, which is apparent to the real images due to the blood flow and scattering effects. The second artificial image is used to simulate the non uniform image background of real infrared images which created by applying an iterative spatial low pass Gaussian filter with a large window size to the original infrared image.

Evaluation Rates

In the finger vein segmentation process, each pixel is classified as tissue (non-vein) or vein. Consequently, there are four events, true positive (*TP*) and true negative (*TN*) when a pixel is correctly segmented as vein or non-vein, and two misclassifications, a false negative *(FN)* appears when a pixel in a vein is segmented in the non-vein area, and a false positive (*FP*) when a non-vein pixel is segmented as a vein pixel.

Two widely known statistical measures are used for method evaluation: sensitivity and specificity, which are used to evaluate the performance of the binary segmentation outcome. The sensitivity is a normalized measure of true positives, while specificity measures the proportion of true negatives:

$$sensitivity = \frac{TP}{TP + FN}, \tag{11}$$

$$specificity = \frac{TN}{TN + FP}. \tag{12}$$

Usually, there is a tradeoff between two measures. Finally, the accuracy of the binary classification is defined by:

$$accuracy = \frac{TP + TN}{P + N}, \tag{13}$$

where *P* and *N* represent the total number of positives (vein) and negatives (non-vein) pixels in the segmentation process and is the degree of conformity of the estimated binary classification to the true according to a manual segmentation. Thus, the accuracy is strongly related to the segmentation quality and for this reason it is used to evaluate and compare different methods.

The proposed method is evaluated quantitatively on the artificial image database. Each image of the set is constructed according to the above procedure. The evaluation is performed using the widely known statistical measures of sensitivity, specificity and accuracy. TABLE 1 shows the mean sensitivity, specificity and accuracy of the proposed method on the artificial finger image database, while FIG. 9 shows the *ROC* curve produced by varying the local segmentation threshold and estimating the corresponding measures.

TABLE 1 MEAN SENSITIVITY, SPECIFICITY AND ACCURACY OF THE PROPOSED METHOD WITHOUT PREPROCESSING/POSTPROCESSING

	Sensitivity	**Specificity**	**Accuracy**
Mean	0.869	0.898	0.892
Standard Deviation	0.081	0.025	0.036

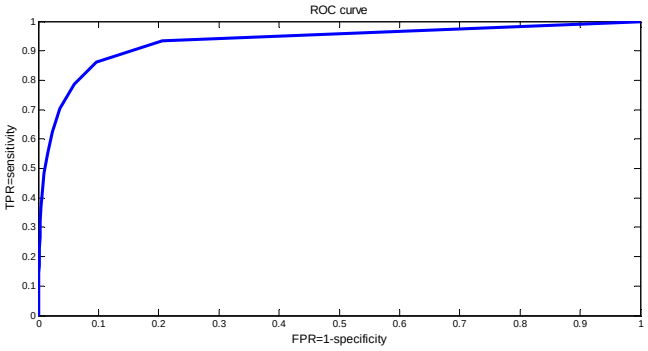

FIG. 9 ROC CURVE OF THE PROPOSED METHOD PRODUCED BY VARYING THE LOCAL SEGMENTATION THRESHOLD

FIG. 10 shows the first image of the artificial image database used for the evaluation of the proposed method and the corresponding result of the segmentation. In these experiments preprocessing and postprocessing steps had not been applied.

FIG. 10 ARTIFICIAL INFRARED FINGER IMAGE AND THE EXTRACTED VEIN PATTERN

Conclusions

In this paper a robust method for finger vein pattern extraction in infrared images is presented and evaluated taking into account the directional

properties of the fingerprint lines and vein patterns. The use of multiple-directional filters combines the steerability principle and the multiscale analysis. Steerable filters based on wavelets, rotated at arbitrary directions, are reliable to derive and separate visual information in infrared images of finger. Although in our evaluation we did not take advantage of the multi-scale version of the algorithm, we referred in the fact that this multi-scale version might ease a lot of similar image processing tasks such as road extraction from satellite images and retinal vessel segmentation. A comparison with other existing methods also enhances the robustness of the one proposed. In addition, the presented method is extended for cases where the noise is evident and the image quality is low by applying the preprocessing and postprocessing steps.

REFERENCES

Ding Y., Zhuang D. and Wang K., "A Study of Hand Vein Recognition Method", Proceedings of the IEEE International Conference on Mechatronics & Automation, Niagara Falls, Canada, July 2005.

Freeman W.T. and Adelson E.H., "The Design and Use of Steerable Filters," IEEE Trans. PAMI, 13(9), September 1991, pp.891-906.

Gongalez R., Woods R., Eddins S., "Digital image processing using matlab", 2003, Prentice Hall.

Hong D.U., Im S.K., and Choi H.S., "Implementation of Real Time System for Personal Identification Algorithm Utilizing Hand Vein Pattern," Proc. of IEEK Fall Conf., 1999, Vol. 22, No. 2, pp. 560-563.

Im S.K., Choi H.S., and Kim S.W., "Direction-Based Vascular Pattern Extraction Algorithm for Hand Vascular Pattern Verification" Korea University, Seoul, Korea. ETRI Journal, Vol. 25, No. 2, April 2003.

Im S.K., Park H.M., and Kim S.W., "A Biometric Identification System by Extracting Hand Vein Patterns," Journal of the Korean Physical Society, Vol. 38, No. 3, 2001, pp. 268-272.

Im S.K., Park H.M., Kim S.W., Chung C.K., and Choi H.S., "Improved Vein Pattern Extracting Algorithm and its Implementation," Proc. of IEEE ICCE, 2000, pp. 2-3.

Mallat S. and Zhong S.,"Characterization of Signals from Multiscale Edges," IEEE Trans. PAMI, 14(7), July 1992, pp.710-732.

Miura N., Nagasaka A., Miyatake T., "Feature extraction of finger-vein patterns based on iterative line tracking and its application to personal identification", Systems and Computers in Japan, Vol. 35, No. 7, 2004.

Miura N., Nagasaka A., Miyatake T., "Feature extraction of finger-vein patterns based on repeated line tracking and its application to personal identification", Machine Vision and Applications (2004) Vol. 15, pp.194-203.

Otsu N., "A threshold selection method from grey-level histograms", IEEE Trans. Syst., Man., Cybern. SMC-9, 62-66 (1979).

Paquit V., Price J.R., Seulin R., Meriaudeau F., Farahi R.H., Tobin K.W. and Ferrell T. L., "Near-infrared imaging and structured light ranging for automatic catheter insertion", Proceedings of the SPIE, Vol. 6141, 2006, pp. 545-553.

Park G.T., Im S.K., and Choi H.S., "A Person Identification Algorithm Utilizing Hand Vein Pattern," Proc. of Korea Signal Processing Conf., Vol. 10, No. 1, 1997, pp. 1107-1110.

Tanaka T., Kubo N., "Biometric Authentication by Hand Vein Patterns", SICE Annual Conference in Sapporo, August 2004.

Vlachos M., and Dermatas E., "A finger vein pattern extraction algorithm based on filtering in multiple directions", 5th European Symposium on Biomedical Engineering, July 2006.

Zeman H.D., Lovhoiden G., and Vrancken C., "Prototype Vein Contrast Enhancer," Proc. SPIE, vol. 5318, in press, 2004.

Zeman H.D., Lovhoiden G., and Vrancken C., "The Clinical Evaluation of Vein Contrast Enhancement", Proc. SPIE, vol. 4615, pp.61-70, 2002.

Marios D. Vlachos was born in Sparti, Greece, in 1981. Currently, he is a freelance-researcher.

He received his Diploma and PhD degrees from the Department of Electrical and Computer Engineering of the University of Patras, Patras, Hellas in 2004 and 2010 respectively.

Dr. Vlachos research interests focus on biomedical image processing and analysis, pattern recognition and biometrics.

Evangelos S. Dermatas is Associate Professor at the Department of Electrical and Computer Engineering of the University of Patras, Patras, Hellas.

He received his Diploma and PhD degrees from the Department of Electrical Engineering of the University of Patras, Patras, Hellas in 1985 and 1991 respectively.

Professor Dermatas research interest areas include: medical imaging, Speech & natural language processing, statistical signal processing, pattern recognition.